Journal of Power Sources 195 (2010) 7511–7516

Contents lists available at ScienceDirect

Journal of Power Sources

journal homepage: www.elsevier.com/locate/jpowsour

Effects of addition of different carbon materials on the electrochemical performance of nickel hydroxide electrode

Agnieszka Sierczynska[a,*], Katarzyna Lota[a], Grzegorz Lota[a,b]

[a] Institute of Non-Ferrous Metals Department in Poznan, Central Laboratory of Batteries and Cells, Forteczna 12, 61-362 Poznan, Poland
[b] Poznan University of Technology, Institute of Chemistry and Technical Electrochemistry, Piotrowo 3, 60-965 Poznan, Poland

ARTICLE INFO

Article history:
Received 15 September 2009
Received in revised form
25 December 2009
Accepted 29 December 2009
Available online 11 January 2010

Keywords:
Ni–MH battery
Positive electrode
Carbon nanotubes
Electrochemical performance

ABSTRACT

Nickel hydroxide is used as an active material in positive electrodes of rechargeable alkaline batteries. The capacity of nickel–metal hydride (Ni–MH) batteries depends on the specific capacity of the positive electrode and utilization of the active material because of the $Ni(OH)_2$/NiOOH electrode capacity limitation. The practical capacity of the positive nickel electrode depends on the efficiency of the conductive network connecting the $Ni(OH)_2$ particle with the current collector. As β-$Ni(OH)_2$ is a kind of semiconductor, the additives are necessary to improve the conductivity between the active material and the current collector. In this study the effect of adding different carbon materials (flake graphite, multi-walled carbon nanotubes (MWNT)) on the electrochemical performance of pasted nickel–foam electrode was established. A method of production of MWNT special type of catalysts had an influence on the performance of the nickel electrodes. The electrochemical tests showed that the electrode with added MWNT (110–170 nm diameter) exhibited better electrochemical properties in the chargeability, specific discharge capacity, active material utilization, discharge voltage and cycling stability. The nickel electrodes with MWNT addition (110–170 nm diameter) have exhibited a specific capacity close to 280 mAh g^{-1} of $Ni(OH)_2$, and the degree of active material utilization was ~96%.

1. Introduction

Alkaline rechargeable batteries, e.g., nickel–metal hydride (Ni–MH), have been used in power tools to portable electronics, UPS, electric vehicles or hybrid electric vehicles. The capacity of Ni–MH batteries depends on the specific capacity of the positive electrode and the utilization of the active material because of the positive electrode capacity limitation. Nickel hydroxide is the active material for cathode material of these batteries. Spherical $Ni(OH)_2$ with a particle size about several microns is used generally. The method of preparation of high density spherical nickel hydroxide has an influence on specific energy and electrochemical performance of nickel electrode [1–3]. The theoretical capacity of nickel hydroxide is 289 mAh g^{-1}, because of one-electron transfer during reaction. The β-$Ni(OH)_2$ is a p-type semiconductor. The main reaction that occurs at the nickel electrode during the charging process: $Ni(OH)_2 + OH^- \leftrightarrow NiOOH + H_2O + e^-$; one proton going to form water and one electron are released on charge at the reaction site within the active material [4,5]. Unfortunately, during charging of electrode, nickel hydroxide can be converted into both forms β and γ. The exact oxidation states of oxyhydroxides (β, γ) are not very strictly specified, showing that the structures of various nickel oxyhydroxides are very complicated [6]. The γ-oxyhydroxide is more difficult to reduce to nickel hydroxide upon discharge process due to its structure created as a consequence of insertion of potassium ions from the electrolyte into interlayer space of the lattice structure [7]. At first, γ-NiOOH is formed at the collector side of the electrode and expanded to the solution side during discharging cycling – this phenomenon is known as a memory effect observed in alkaline rechargeable batteries [8].

Poor conductivity of active material $Ni(OH)_2$/NiOOH requires addition of some additives to increase conductivity. Co or Co compounds have been used as conductive additives to positive electrode and additionally to increase the oxygen evolution potential, the charge efficiency and to inhibit the development of γ-NiOOH structure order. The effect of addition of cobalt is also in improving mechanical properties of nickel electrodes [7,9–12]. The carbonaceous materials such as graphite and acetylene black are also used to improve the conductivity and material utilization of the electrode [13–15]. Also carbon nanotubes were used as a functional additive to improve the electrochemical performance of pasted nickel foam electrodes [16–18]. The improvement of material utilization and specific discharge capacity of nickel electrode with MWNTs is connected with lower electrochemical impedance and less γ-NiOOH forming during charge/discharge cycling.

* Corresponding author. Tel.: +48 61 2797892; fax: +48 61 2797897.
E-mail addresses: sierczynska@claio.poznan.pl (A. Sierczynska), lota@claio.poznan.pl (K. Lota), grzegorz.lota@put.poznan.pl (G. Lota).

0378-7753/$ – see front matter © 2010 Elsevier B.V. All rights reserved.
doi:10.1016/j.jpowsour.2009.12.094

Table 1
BET surface areas of carbon additives.

Sample	Additives of carbon materials				
	Graphite	MWNT 110–170 nm	MWNT 110–170 nm mod.[a]	MWNT 10–15 nm	MWNT 10–15 nm mod.[a]
BET surface area ($m^2\ g^{-1}$)	5	18	12	137	220

[a] mod. means after modification.

This paper presents a comparative study carried out on five different carbonaceous materials as additives to active material of the nickel electrode.

2. Experimental

The $Ni(OH)_2$/NiOOH electrodes were prepared with commercial spherical β-$Ni(OH)_2$ powder as an active material and addition of metallic cobalt powder, calcium oxide and various carbon materials to improve the electrochemical properties.

To evaluate the electrochemical properties of the pasted nickel hydroxide electrodes, they were prepared as follows: 88% $Ni(OH)_2$ (Hoboken), 7% carbon material, 3% Co (Eurotungstene) and 2% CaO (Aldrich). As carbon materials were used: graphite KS 5–75 μm (Lonza), MWNT O.D. 10–15 nm (Aldrich) – purity >90% and MWNT O.D. 110–170 nm (Aldrich) – purity >90%. Additionally, MWNT were modified by acidic treatment (concentrated hydrochloric acid) to remove metallic impurities. All materials before and after modification were tested as a conductive additive to nickel electrode. All components were mixed thoroughly, and 3 wt.% suspension containing 60 wt.% polytetrafluoroethylene (PTFE) and 1.5 wt.% polyhydroxymethylcellulose (HPMC) was added to the mixed powder as a binder. The mixture was then blended to obtain paste and it was pasted into nickel foam to form a 1 cm × 1 cm electrode. After drying at 70 °C for 12 h, the pasted electrode was pressed to assure good electrical contact between the substrate and the active material.

The carbonaceous materials and electrodes with these additives were characterized by scanning electron microscopy (SEM EVO®40 ZEISS). Specific surface area measurements were performed using ASAP 2010 M (Micromeritics).

The electrochemical properties, such as a specific capacity, charge efficiency, percent of utilization and cycleability were characterized by the galvanostatic charge/discharge cycling, cyclic voltammetry and electrochemical impedance spectroscopy in the half-cells. The electrochemical measurements were carried with a classical three-compartment glass cell containing 6 M KOH solution as electrolyte. The working $Ni(OH)_2$/NiOOH electrode was soaked in the electrolyte solution for 12 h before test. A hydrogen-storage alloy electrode ($LaNi_5$ type) with capacity well in excess of the nickel electrodes was used as a counter electrode. For the reference electrode, a Hg/HgO/6 M KOH electrode was employed. All potentials in this paper are reported with reference to the latter electrode. The measurements were performed at room temperature. During the 1st cycle the charge process was conduced till the beginning of the oxygen evolution on electrode. In the subsequent cycles the electrode was charged up to 120% of the electrode capacity in relation to discharge capacity of the 1st cycle. The charge process for the 1–10 cycles were performed at a rate of 0.1 C, while 11–50 cycles the charge was performed at a rate of 0.2 C. After one

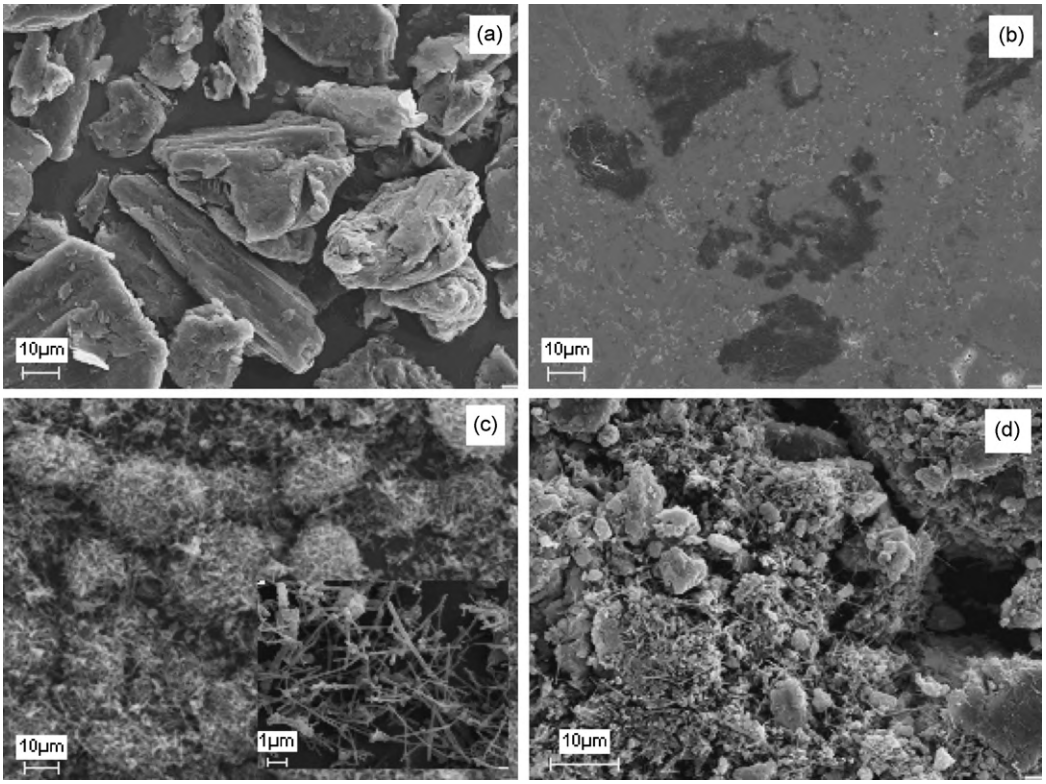

Fig. 1. SEM images of: (a) flake graphite KS 5–75 μm; (b) nickel electrode with flake graphite KS 5–75 μm addition; (c) MWNT 110–170 nm; (d) nickel electrode with MWNT 110–170 nm addition.

hour of a rest period for potential equilibration the electrode was discharged at 0.2 C to the potential 0.18 V vs. Hg/HgO. The galvanostatic charge/discharge measurements were made with Battery Testing Equipment Atlas-Sollich.

For the electrochemical impedance spectroscopy (EIS) measurement the nickel electrodes were activated by charge/discharge cycling before experiments, and the spectra were recorded at a 5 mV amplitude of perturbation with a sweep frequency range from 100 kHz to 10 mHz, and at opened circuit potential (OCP). The electrochemical impedance spectroscopy (EIS) and the cyclic voltammetry (CV) tests were performed using an Autolab PGSTAT 30/FRA2 system.

3. Results and discussion

3.1. Characterization of electrodes with carbon materials

The results of BET surface measurements of carbonaceous additives are shown in Table 1. The carbonaceous materials used as conductive additives varied in the surface area (from 5 $m^2 g^{-1}$ to 220 $m^2 g^{-1}$) and particle size distribution. The MWNT 10–15 nm show the highest BET surface area because of the highest value of microporosity, which is a main factor of a considerable surface area. The electrode with flake graphite is characterized by quite good electrochemical performance and forms a base to comparison studies. The addition of 7 wt.% of carbonaceous material was chosen for easy comparison of the electrochemical performance of this electrode.

The scanning electron microscopy images were performed on carbon materials: flake graphite and MWNT 110–170 nm and electrodes with these additives are shown in Fig. 1. We can observe the scaly structure of graphite (Fig. 1a) and probably distinguish the shape of graphite flakes on the surface of pressed electrode (Fig. 1b). The flake graphite is characterized by size of particles between 5 μm and 75 μm. The outer diameter of commercial carbon nanaotubes, as we can see in Fig. 1c, is between 100 nm and 200 nm and several micrometers in length. MWNT create network for particles of spherical nickel hydroxide. Because of very good mechanical properties such as high elastic modulus and bending strength, MWNT do not surrender to the pressure easily and they lowered the packing density of $Ni(OH)_2$ particles in three-dimensional porous nickel foam. Such a kind of network prevents extension and shrinkage of nickel electrode, because it is well known that positive electrode lose active material from support during cycling charging/discharging. MWNT prevent volume variations.

Both types of MWNT were additionally modified, to remove the rest of metallic catalyst applied in process production of these materials. The process of modification was made in the concentrated HCl, at 80 °C. The mixture was stirred intensely for 12 h for a more effective dissolution of metallic components. To estimate MWNT impurities, chemical composition of the HCl solution used for modification of MWNT was determined by inductively coupled plasma spectroscopy (ICP). ICP analysis was performed to determine the amount of each element dissolved in acidic solution.

The results of analysis are shown in Table 2. The main reason for the big difference between metallic impurities (Ni, Co, Fe, etc.) is that each kind of carbon nanotubes was produced using different catalysts. The method of carbon nanotubes preparation (especially catalysts) has a huge influence on a structure and properties of the carbon deposit.

Table 2
Amount of elements dissolved in HCl solution after modification of MWNT.

Dissolved amount of element (wt.%)	Additives of carbon materials	
	MWNT 110–170 nm mod.[a]	MWNT 10–15 nm mod.[a]
Ni	0.270	0.020
Co	0.090	0.030
Fe	0.090	0.700
Mg	0.016	0.016
Li	0.013	0.003
Cu	0.008	0.010
Mn	0.020	0.007

[a] mod. means after modification.

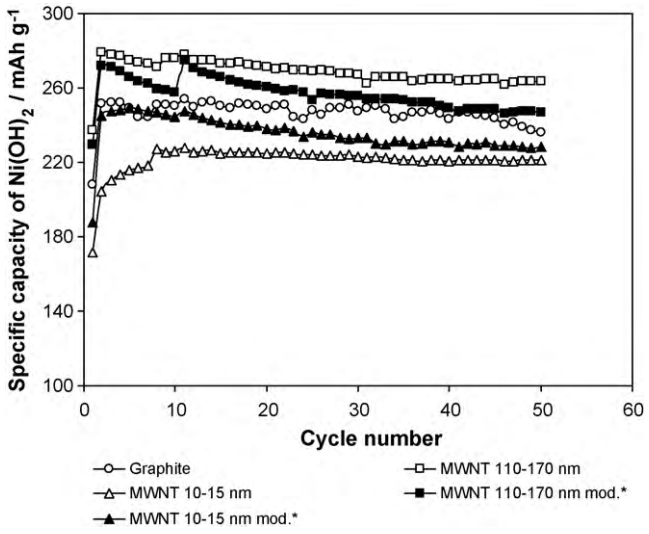

Fig. 2. Cycling stability of the nickel electrodes with different carbon materials addition calculated on mass of nickel hydroxide.

3.2. Cycling stability of pasted nickel electrodes

To evaluate the practical effects of addition different carbon materials, the galvanostatic charge/discharge tests were performed, which are shown in Fig. 2.

All the curves present stable specific discharge capacity in followed 50 cycles. The electrode with MWNT 110–170 exhibits the highest specific capacity with very good cycling stability. The specific capacity (mAh g^{-1} of $Ni(OH)_2$) of that electrode dropped slightly from 276 in the 3rd cycle to 264 in the 50th cycle (less than 5%). The highest drop of capacity (15%) in 50th cycle is observed for electrode with modified MWNT 10–15 nm. The sharp increase of the specific capacity for all nickel electrodes around 10th cycle is connected with changing the condition of the charge process. The 1–10 cycles were performed at a rate of 0.1 C, while 11–50 cycles the charge was performed at a rate of 0.2 C. The electrode

Table 3
Comparison of the maximal specific capacity and the utilization of $Ni(OH)_2$ in positive electrodes with different carbon materials.

Sample	Additives of carbon materials				
	Graphite	MWNT 110–170 nm	MWNT 110–170 nm mod.[a]	MWNT 10–15 nm	MWNT 10–15 nm mod.[a]
Maximal specific capacity (mAh g^{-1})	254.9	276.4	271.1	235.5	244.0
Utilization ratio of β-$Ni(OH)_2$ (%)	88.2	95.6	93.8	81.5	84.5

[a] mod. means after modification.

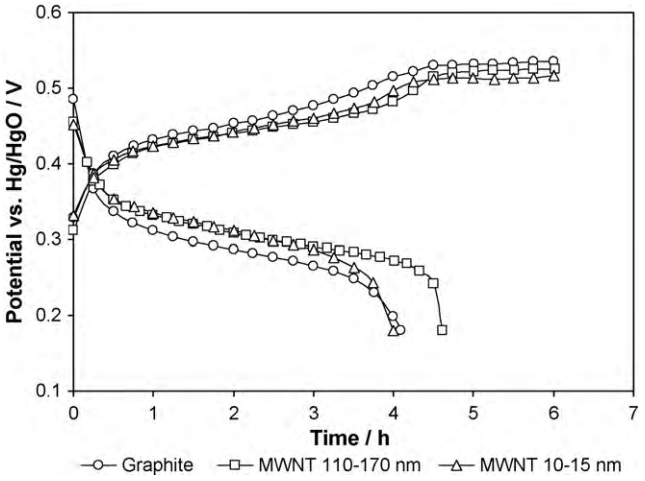

Fig. 3. Charge/discharge curves registered during the 3rd cycle.

was discharged at 0.2 C. The most visible changes after modification of the charging conditions are for the electrode with addition MWNT 110–170 nm after modification.

Regardless of the mass of other compounds of nickel electrode the maximal specific capacity of $Ni(OH)_2$ is shown in Table 3.

As we can see, the specific capacity of materials after modification (HCl treatment) is different for both kinds of carbon nanotubes. It is probably connected with various kinds of catalyst used for their production. In the case of MWNT 10–15 nm after acid treatment, they are characterized by better electrochemical properties mainly due to the fact that iron (the rest of catalyst) was dissolved. The presence of iron (which can create (α-FeOOH)) can lead to the occurrence of a concurrent reaction on the nickel electrode [19]. In addition, such a kind of modification probably improves the hydrophilic of material and it can be more accessible for an electrolyte. Whereas dissolving nickel and cobalt in HCl (metals which are usually added to active mass of nickel electrode) from MWNT 110–170 nm leads to worsening capacitive parameters.

In addition, the electrodes with graphite and MWNT 110–170 nm before and after modification obtain their top specific capacity in the 3rd cycle, whereas the electrode with MWNT which have about 10–15 nm in outer diameter obtain their maximum capacity before modification approximately in 10th cycle, and after acid treatment in the 5th cycle. This kind of modification probably improves the hydrophilic of material and it can be more accessible for electrolyte.

Fig. 3 shows typical charge and discharge curves for the pasted nickel electrodes with different carbon materials, the rates for all the charge are 0.1 C and discharge is 0.2 C. Both types of MWNT reduce the oxidizing and reducing potentials of nickel electrode and increase the overpotential of oxygen evolution. The top-of-charge voltages of electrodes with MWNT are lower than that of electrode with graphite, which implies that such kind of additives improve chargeability and lower intrinsic resistance. The discharge time of electrode with MWNT 110–170 nm is longer than that of electrodes with graphite and MWNT 10–15 nm and the plateau of electrode with MWTN 110–170 nm is also higher and flatter than residual electrodes.

3.3. EIS and CV measurements of pasted nickel electrodes

Given these findings, it can be concluded that the nickel electrode with added MWNT 110–170 nm indicated less polarization during the charge/discharge process comparing with the electrode with graphite, which is confirmed by the EIS study. Fig. 4 presents the electrochemical impedance spectra for electrodes with different carbon materials.

Kinetics of nickel electrode is mainly assigned by solid-state proton insertion reaction. That is why its impedance can be considered as that of insertion material, that is proton diffusion toward the center of solid-state particles and specific conductivity of the porous material itself [20]. The EIS spectra of pasted electrodes after 10th and 50th cycles display a depressed semicircle connected with charge transfer resistance in the region of high frequencies and slope related to the Warburg impedance (which is strictly connected with diffusion resistance) in the region of low frequencies. It is evident that the charge transfer resistance of electrode with added MWNT 110–170 nm is the smallest both in the 10th and in the 50th cycle. Whereas the electrode with added MWNT 10–15 nm is characterized by the highest value of charge transfer resistance, which during the cycling became bigger, which implies that the electrochemical reaction on such a kind of electrode worsened.

The MWNT 110–170 nm have the optimal size to a shorter current conducting pathway in the active material, which influences a lower internal resistance of electrode.

Cyclic voltammograms for the nickel electrodes with different carbon materials are shown in Fig. 5. For each electrode oxidation/reduction cycles were made in the potential range $E^\circ \rightarrow 0.62\,V \rightarrow 0\,V \rightarrow E^\circ$ vs. Hg/HgO/6 M KOH (E° – the rest potential) at a scan rate of 0.1 mV s^{-1}.

The experimental data obtained from the cyclic voltammetric study are summarized in Table 4. It can be seen that the first anodic peak corresponding to the hydroxide oxidation of electrodes and

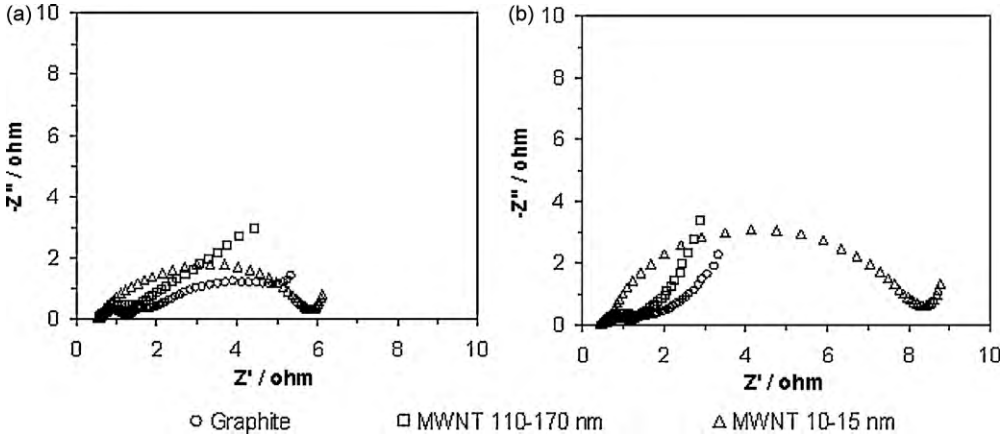

Fig. 4. Electrochemical impedance spectra of pasted nickel electrodes: (a) after 10th cycle; (b) after 50th cycle.

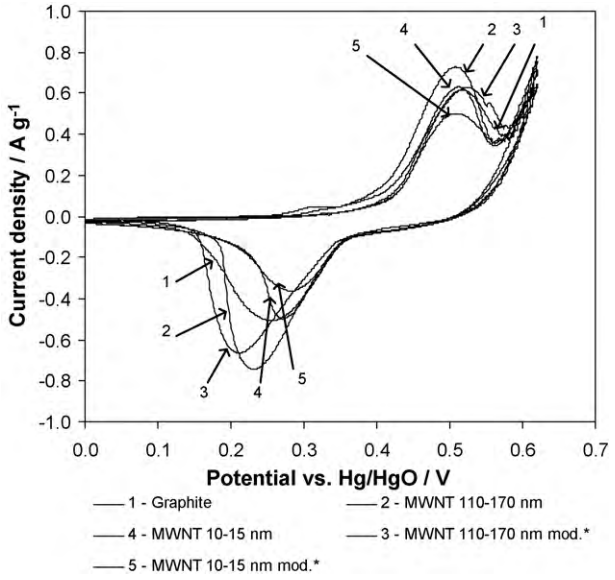

Fig. 5. Cyclic voltammograms of nickel electrodes with different carbon materials ($E^{\circ} \rightarrow 0.62\,V \rightarrow 0\,V \rightarrow E^{\circ}$; $dV/dt = 0.1\,mV\,s^{-1}$).

the second one to oxygen evolution while cathodic peak corresponding to the oxyhydroxide reduction. The oxidation potentials of nickel electrodes with carbon nanotubes before and after modification are different. It is a result of dissolving metallic remainders from carbon materials. In the case of MWNT 110–170 nm it was mainly nickel, while for MWNT 10–15 nm it was iron.

To take into account the mass of electrode, both the anodic and cathodic peak current densities for electrode with MWNT 110–170 nm are higher than those of the rest of the electrodes.

The E_1 and E_2 symbols are employed as the symbol of the potential of anodic and cathodic peak, respectively. The $\Delta E_{1,2}$ symbol, the difference between the anodic and cathodic peak position, is taken as an estimate of reversibility of the redox reaction, which is an important parameter to estimate the electrochemical properties of the electrodes. The smaller a $\Delta E_{1,2}$ is, the more reversible the electrochemical reaction and better proton diffusion efficiency are [21,22]. The results in Table 4 show that the smallest value $\Delta E_{1,2}$, 0.226 V and 0.240 V were obtained for the electrodes with additive MWNT 10–15 nm mod.* and MWNT 10–15 nm, respectively. Whereas for electrode with added MWNT 110–170 nm oxidation potential of Ni(II) is at a less positive potentials. Usually, the charge efficiency decreases as the oxidation potential increases because of concurrent oxygen evolution. Addition of MWNT 110–170 nm allows charging at less positive potentials comparing to others examined additives, less oxygen is evolved and higher charge efficiency is obtained.

Fig. 6 shows the high-rate capability of electrodes with the addition of graphite and MWNT 110–170 nm, in which the efficiency means the ratio of the capacity at various rates to the capacity at the 0.2 C rate. The experimental results show that addition of multi-walled carbon nanotubes (110–170 nm diameter) can considerably enhance the high-rate discharge efficiency of pasted nickel electrodes, and the effects become more remarkable with an increase in the discharge rate. The efficiency of electrode with MWNT 110–170 nm at the rate 2 C is almost twice higher than in the case of electrode with graphite. This indicates that the addition of MWNT 110–170 nm to spherical $Ni(OH)_2$ not only increases the discharge capacity and utilization of nickel hydroxide active material, but also improves the discharge voltage and high-rate capability of nickel electrodes. Given these findings, it can be concluded that the nickel electrode with added MWNT 110–170 nm shows less polarization during the charge/discharge process compared with the electrode with graphite flakes.

Table 4
Potentials of oxidation and reductions peaks.

Additives of carbon materials	E_1 (V)	E_2 (V)	$\Delta E_{1,2}$ (V)
Graphite	0.518	0.255	0.263
MWNT 110–170 nm	0.508	0.232	0.276
MWNT 110–170 nm mod.[a]	0.524	0.211	0.313
MWNT 10–15 nm	0.513	0.273	0.240
MWNT 10–15 nm mod.[a]	0.509	0.283	0.226

E_1 – oxidation potential of Ni (II); E_2 – reduction potential; $\Delta E_{1,2} = E_1 - E_2$.
[a] mod. means after modification.

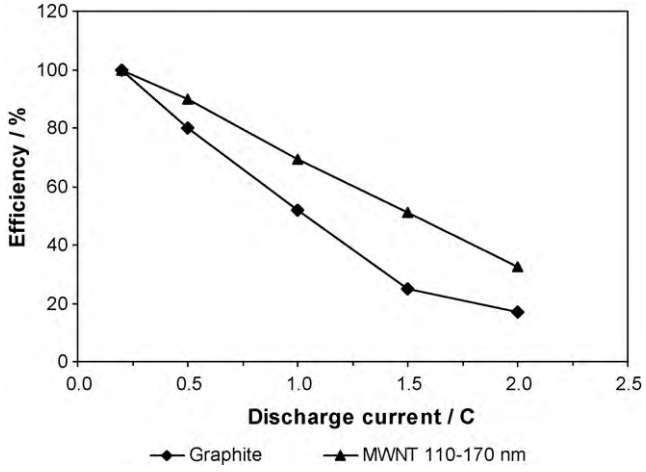

Fig. 6. High-rate capability of pasted nickel electrodes with different carbon materials addition.

4. Conclusions

Multi-walled carbon nanotubes have been used as a functional additive to improve the electrochemical performance of pasted nickel–foam electrodes for rechargeable alkaline batteries. Studies show that addition of MWNT 110–170 nm increases the material utilization and specific discharge capacity as well as improves the discharge voltage and high-rate capability of nickel electrodes. The nickel electrodes with MWNT addition (110–170 nm diameter) have exhibited a specific capacity close to 280 mAh g^{-1} of $Ni(OH)_2$, and the degree of active material utilization was ~96%. The adding of MWNT provides a good electron conductive network between the $Ni(OH)_2$ particles, which results in a shorter current conducting pathway in the active material and a lower internal resistance for the positive electrode and therefore improves the life cycle of the Ni–MH batteries.

Modification of carbon nanotubes proposed in this study had a negligible influence on the performance of nickel electrodes which were obtained during the half-cells measurements. The influence of MWNT modification process was different for both types of carbon nanotubes, which is connected with various catalysts used for carbon materials production. The addition of non-modified MWNT (110–170 nm diameter) exhibited the best electrochemical properties in the chargeability, specific discharge capacity (approaching to the theoretical value), active material utilization, discharge voltage and cycling stability.

The MWNT 10–15 nm show the worse electrochemical characteristic because there is a problem with remainders of catalyst used for their production. In the case of MWNT 10–15 nm after acid treatment, they are characterized by better electrochemical properties mainly due to the fact that iron (rest of catalyst) was dissolved.

Acknowledgement

The financial support by DS 419/E-138/F/2008 and DS 419/E-138/S/2009 is gratefully acknowledged.

References

[1] U. Kohler, C. Antonious, P. Bauerlein, J. Power Sources 127 (2004) 45–52.
[2] Ch. Zhaorong, L. Gongan, Z. Yujuan, Ch. Jianguo, D. Yunchang, J. Power Sources 74 (1998) 252–254.
[3] D. Assumpcao Bertuol, A. Moura Bernardes, J.A. Soares Tenorio, J. Power Sources 193 (2009) 914–923.
[4] H. Bode, K. Dehmelt, J. Witte, Electrochim. Acta 11 (1966) 1079–1087.
[5] Y. Mo, E. Hwang, D.A. Scherson, J. Electrochem. Soc. 143 (1996) 37–43.
[6] C.C. Hu, K.H. Chang, T.Y. Hsu, J. Electrochem. Soc. 155 (2008) F196–F200.
[7] H.H. Law, J. Sapjeta, J. Electrochem. Soc. 136 (1989) 1603–1606.
[8] Y. Sato, S. Takeuchi, K. Kobayakawa, J. Power Sources 93 (2001) 20–24.
[9] Ch. Yang, Int. J. Hydrogen Energy 27 (2002) 1071–1081.
[10] S. Nathira Begum, V.S. Muralidharan, C. Ahmed Basha, Int. J. Hydrogen Energy 34 (2009) 1548–1555.
[11] J.B. Wu, J.P. Tu, T.A. Han, Y.Z. Yang, W.K. Zhang, X.B. Zhao, J. Power Sources 156 (2006) 667–672.
[12] D. Yunchang, L. Hui, Y. Jiongliang, Ch. Zhaorong, J. Power Sources 56 (1995) 115–119.
[13] D. Yunchang, Y. Jiongliang, L. Hui, Ch. Zhaorong, W. Zeyun, J. Power Sources 56 (1995) 201–204.
[14] M. Casas-Cabanas, J.C. Hernandez, V. Gil, M.L. Soria, M.R. Palacin, J. Power Sources 134 (2004) 298–307.
[15] X. Liu, L. Yu, J. Power Sources 128 (2004) 326–330.
[16] Q.S. Song, G.K. Aravindaraj, H. Sultana, S.L.I. Chan, Electrochim. Acta 53 (2007) 1890–1896.
[17] J.B. Wu, J.P. Tu, T.A. Han, Z. Yu, W.K. Zhang, H. Huang, J. Alloys Compd. 449 (2008) 349–352.
[18] J. Lv, J.P. Tu, W.K. Zhang, J.B. Wu, H.M. Wu, B. Zhang, J. Power Sources 132 (2004) 282–287.
[19] D. Yunchang, Y. Jiongliang, Ch. Zhaorong, J. Power Sources 69 (1997) 47–54.
[20] E. Barsoukov, J.R. Macdonald, Impedance Spectroscopy Theory, Experiment, and Application, second ed., John Wiley & Sons Inc., New Jersey, 2005.
[21] C.Y. Wang, S. Zhong, D.H. Bradhurst, H.K. Liu, S.X. Dou, J. Alloys Compd. 330–332 (2002) 802–805.
[22] W. Zhang, W. Jiang, L. Yu, G. Zhang, Z. Fu, W. Xia, M. Yang, Int. J. Hydrogen Energy 34 (2009) 473–480.